POLITECNICO DI TORINO
Repository ISTITUZIONALE

Predicting loss in magnetic steels under arbitrary induction waveform and with minor hysteresis loops

Original
Predicting loss in magnetic steels under arbitrary induction waveform and with minor hysteresis loops / Barbisio, E., Fiorillo, F., Ragusa, C.S.. - In: IEEE TRANSACTIONS ON MAGNETICS. - ISSN 0018-9464. - 40:(2004), pp. 1810-1819. [10.1109/TMAG.2004.830510]

Availability:
This version is available at: 11583/1662364 since:

Publisher:
IEEE

Published
DOI:10.1109/TMAG.2004.830510

Terms of use:

This article is made available under terms and conditions as specified in the corresponding bibliographic description in the repository

Publisher copyright

(Article begins on next page)

18 November 2026

Predicting Loss in Magnetic Steels Under Arbitrary Induction Waveform and With Minor Hysteresis Loops

Edoardo Barbisio, Fausto Fiorillo, and Carlo Ragusa

***Abstract*—We have studied ways of predicting power losses in soft magnetic laminations for generic time dependence of the periodic magnetic polarization $J(t)$. We found that, whatever the frequency and the induction waveform, the loss behavior can be quantitatively assessed within the theoretical framework of the statistical loss model. The prediction requires a limited set of preemptive experimental data, depending on whether or not the arbitrary $J(t)$ waveform is endowed with local slope inversions (i.e., minor hysteresis loops) in its periodic time behavior. In the absence of minor loops, such data reduce, for any peak polarization value $J_{\rm p}$, to the loss figures obtained under sinusoidal $J(t)$ at two different frequency values. In the presence of minor loops of semiamplitude $J_{\rm m}$, the two-frequency loss experiment should be carried out for both peak polarization values $J_{\rm p}$ and $J_{\rm m}$. Additional knowledge of the quasi-static major loop, to be used for modeling hysteresis loss, does improve the accuracy of the prediction method. A more general approach to loss in soft magnetic laminations is obtained in this way, the only limitation apparently being the onset of skin effect at high frequencies.**

***Index Terms*—Eddy currents, magnetic losses, Preisach models of magnetic hysteresis, soft magnetic materials.**

I. Introduction

SOFT magnetic materials are classified, sold, and applied on the basis of the properties determined by means of standard test methods. AC magnetic testing made according to the standards invariably requires sinusoidal induction, quite a natural working condition in magnetic cores. On the one hand, such are the typically rated voltages in electrical machines and devices and, on the other hand, there is an obvious basic aspect attached to sinusoidal induction waveforms, as building blocks of any possible periodic function. It frequently happens, however, that practical magnetic cores or substantial portions of them are subjected to nonsinusoidal flux. In some cases one can talk of distortion, that is unwanted departure from the ideal sinusoidal condition due to causes like strong nonlinearity of the material at high inductions, anisotropy (T-joints of transformers), and pulsating waveforms (teeth of stator cores). In other instances, like in variable speed motors supplied by means of pulsewidth modulated (PWM) voltages, the driving circuit itself generates nonsinusoidal flux and the core losses are drastically increased [1]. One is thus faced with the problem of calculating or at least estimating the influence of distortion or modulation on the loss behavior of the magnetic cores, starting from information on the material properties obtained by means of standard testing. The characterization of the material under controlled nonconventional exciting conditions, while made easier by increasingly available digital measuring systems, is still matter for specialized laboratories. On the other hand, dealing with the large variety of practically encountered waveforms would be a big experimental burden, requiring, for example, the creation of a large database for any specific material or, yielding to apparent predicting inability, even the difficult and ambiguous identification of benchmark induction waveforms, on which a new measuring standard might possibly be built [2]. Data sheets from manufacturers typically report the loss figure of the materials, obtained at power frequencies (50–60 Hz) for selected peak induction values. In some cases, quasi-static hysteresis loops are also available. Altogether, these data are deemed to convey relatively poor information for the sake of predictive purposes, but there cannot be an objective way to define minimum base information without a sound physically based theoretical loss model. This kind of model was introduced some years ago [3], based on the *statistical theory of losses* [4]. It can be applied, in somewhat simplified form, to the prediction of power losses in soft magnetic laminations under sinusoidal and nonsinusoidal induction waveform, provided the working frequency is sufficiently low to ensure uniform flux penetration (no skin effect). A number of investigations in the literature have proved its good predicting power in different materials and with different waveforms [5]–[7], as well as the limitations provided by the appearance of the skin effect [8]. The model relies on the physically based idea of loss separation, where the total average power loss $P(f)$ at a given frequency f is expressed as the sum of the hysteresis $P_{\rm h}(f)$, classical $P_{\rm cl}(f)$, and excess $P_{\rm exc}(f)$ components

$$P(f) = P_{\rm h}(f) + P_{\rm cl}(f) + P_{\rm exc}(f) \tag{1}$$

where $P_{\rm h}(f) = W_{\rm h} f$, $W_{\rm h}$ is the hysteresis energy loss per cycle. Except for a few special cases [9], $W_{\rm h}$ is always considered as a frequency-independent quantity. Equation (1) can then equivalently be written in terms of the energy loss per cycle $W = P/f$

$$W(f) = W_{\rm h} + W_{\rm cl}(f) + W_{\rm exc}(f). \tag{2}$$

The model can be applied in principle to whatever induction waveshape, but some limitations may occur because of the

Manuscript received February 26, 2004; revised April 5, 2004. This work was supported in part by the Italian Ministry of Education, University and Research (MIUR) under Grant MM09321847.

E. Barbisio and C. Ragusa are with the Dipartimento di Ingegneria Elettrica Industriale, Politecnico di Torino, Torino I-10129, Italy (e-mail: Edoardo.Barbisio@polito.it; Carlo.Ragusa@polito.it).

F. Fiorillo is with the Istituto Elettrotecnico Nazionale (IEN) Galileo Ferraris, 10135 Torino, Italy (e-mail: fiorillo@ien.it).

Digital Object Identifier 10.1109/TMAG.2004.830510

0018-9464/04$20.00 © 2004 IEEE

simplifications introduced in the original derivation of it [3], while, at the same time, application to the relatively complex case where induction versus time shows local slope inversions (or, equivalently, hysteresis is characterized by the presence of minor loops) has yet to be made. Other methods of loss prediction under distorted induction, with or without minor loops, have actually been proposed in the recent and less recent literature [10]–[15]. They have limited predicting capability, because they do generally fail to consider loss separation in the right perspective and lack any general analytical formulation. In this paper, we describe how the previously mentioned model can be made general to the point of predicting power losses in magnetic laminations under arbitrary induction waveform and minor loops. Depending on the amount of available preemptive information, it can be applied to different levels of complexity and accuracy. Actually, in order to obtain a satisfactorily general prediction at a given peak magnetization $J_{\rm p}$, we cannot exclusively rely on the experimental knowledge of the total losses measured under standard conditions at a given frequency (e.g., 50–60 Hz). But, it happens very frequently that this is the sole information available from the material manufacturers.

In the absence of minor loops, at least one further total loss value at a different frequency should additionally be known. Alternatively, the quasi-static hysteresis loop or, better, the total energy loss $W(f)$ versus frequency f behavior in a convenient frequency range (e.g., 1–50 Hz) for triangular or sinusoidal induction should be determined.

If the magnetization versus time behavior contains local slope inversions, that is the associated hysteresis loop contains minor loops, we need, in order to preserve good predicting accuracy, another piece of information. It is expedient to assume that the loss characteristic parameters for a symmetrical major loop of $J_{\rm M}$ amplitude (whose determination requires, at least, a two-frequency measurement) and for a 2 $J_{\rm m}$ peak-to-peak minor loop, wherever its branching occurs, are the same. Therefore, a record of two-frequency tests, performed on symmetric magnetization loops of selected amplitude, will give the interpolation support for any intermediate minor loop contents.

II. Theoretical Analysis

The separation procedure outlined in (1) and (2), which can be fully justified from the physical viewpoint [16], is the methodological key to the general prediction of energy losses, because it permits one to pursue this fundamental objective by separately considering the frequency-independent $W_{\rm h}$ and the frequency-dependent $W_{\rm cl}, W_{\rm exc}$ terms. Let us therefore see how this method can be implemented in the practical case of soft magnetic laminations subjected to periodic law of magnetization $J(t)$ of unrestricted shape and given peak amplitude $J_{\rm p}$.

A. Energy Losses With Arbitrary Flux Waveform and No Minor Loops

This problem was considered in [3]. We will generalize here the related theoretical approach, illustrating its application to few practical examples in soft magnetic laminations. Basically, the model relies on the concept of *instantaneous* power loss and loss separation equations, which give physical meaning by detailed analysis of the magnetization process [16].

1) Quasi-Static Loss Component: In the absence of minor loops, the hysteresis energy loss $W_{\rm h}$ is independent of the induction waveshape, for the very same physical reason making it independent of the magnetization rate.

2) Classical Dynamic Loss Component: The instantaneous classical power loss per unit volume $p_{\rm cl}(t)$, due to eddy currents, can be defined for a magnetic lamination of conductivity σ and thickness d as

$$p_{\rm cl}(t) = \frac{1}{12}\sigma d^2 \dot{B}^2(t) \cong \frac{1}{12}\sigma d^2 \dot{j}^2(t) \tag{3}$$

where $\dot{J}(t)$ is the time derivative of the magnetic polarization (in deriving theoretical formulations for magnetic energy losses in soft magnets, distinction is not made, in general, between induction B and magnetic polarization J). The classical energy loss per cycle is then obtained as

$$W_{\rm cl} = \int_0^T p_{\rm cl}(t)\,{\rm d}t = \frac{1}{12}\sigma d^2 \int_0^T J^2(t)\,{\rm d}t \tag{4}$$

and it can be, in principle, exactly calculated under whatever $J(t)$ law, including waveforms with local minima.

Otherwise, by knowing the $J(t)$ harmonic content, instead of (4), one could use

$$W_{\rm cl} = \frac{\pi^2}{6}\sigma d^2 f \sum_{\rm n} n^2 J_{\rm n}^2 \tag{5}$$

where J_n is the peak amplitude of the harmonic component of order n.

The problem of loss prediction under generic $J(t)$ law, apart from the actual difficulty of the $W_{\rm cl}$ evaluation (to be carried out on the basis of (4) or (5), whichever is the simplest algorithm), consists in the prediction of the excess loss component $W_{\rm exc}(f)$.

3) Excess Dynamic Loss Component: We need to define an expression for the instantaneous excess power loss $p_{\rm exc}(t)$, which, integrated over the period $T = 1/f$, could predict the quantity $W_{\rm exc}(f)$ [3]. Such an expression is derived from Bertotti's statistical theory of losses [4], [16], which provides, for a wide class of materials [17], the equation

$$p_{\rm exc}(t) = \frac{n_{\rm o}V_{\rm o}}{2}\left(\sqrt{1+\frac{4\sigma GSV_{\rm o}}{n_{\rm o}^2V_{\rm o}^2}|\dot{J}(t)|}-1\right)|\dot{J}(t)| \tag{6}$$

where $n_{\rm o}$ is the number of simultaneously active magnetic objects (magnetically correlated regions in the sample cross section, as defined and discussed in [4]) in the limit $f \to 0$, $V_{\rm o}$ is a parameter defining the statistics of the magnetic objects, $G = 0.1356$ is a dimensionless coefficient, and S is the cross-sectional area of the lamination. It is stressed that $V_{\rm o}$ and $n_{\rm o}$, which lump the effect on the excess loss of the material structure, depend on $J_{\rm p}$. It can often be assumed that

$$\frac{4\sigma GSV_{\rm o}}{n_{\rm o}^2V_{\rm o}^2}|\dot{J}(t)| \gg 1. \tag{7}$$

Equation (6) consequently reduces to

$$p_{\rm exc}(t) = \sqrt{\sigma GSV_{\rm o}}|\dot{J}(t)|^{3/2} \tag{8}$$

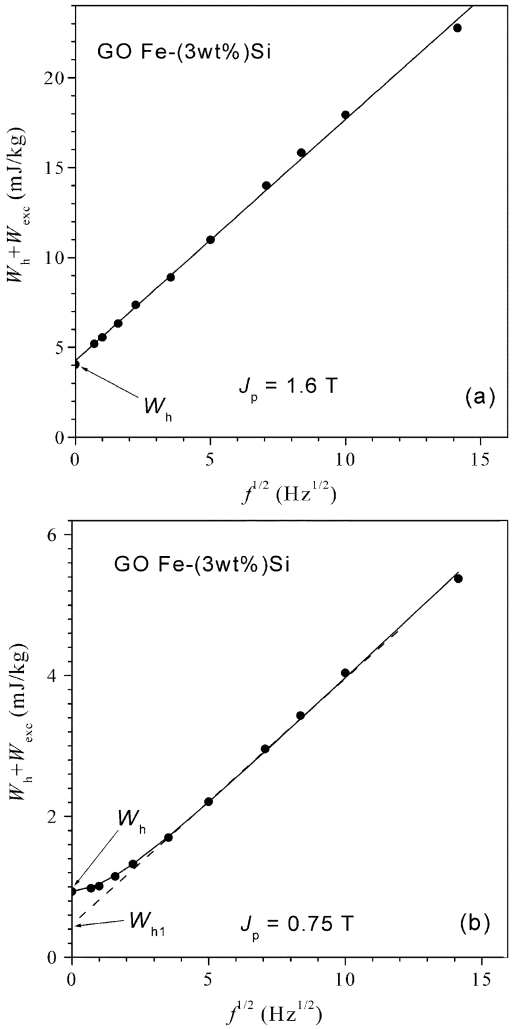


Fig. 1. Examples of experimental dependence of the quantity $W_{\rm dif} = W - W_{\rm cl} = W_{\rm h} + W_{\rm exc}$ on the square root of frequency in grain-oriented Fe–Si laminations (thickness 0.29 mm). The zero-frequency value $W_{\rm dif}(0) = W_{\rm h}$ is in these experiments directly determined by means of a ballistic measurement and all the other points are obtained from measurements under sinusoidal flux. $W_{\rm cl}$ can always be calculated exactly, whatever the flux waveform and the prediction problem is eventually focused on $W_{\rm exc}$. This is everywhere proportional to $\sqrt{f}$ at high inductions (a), while it deviates from linearity at very low frequencies (less than few hertz) at intermediate and low inductions (b). These behaviors are theoretically predicted by (10) and (15), respectively. The dashed straight line in (b) is given by (22).

and the excess energy loss

$$W_{\rm exc} = \int_0^T p_{\rm exc}(t)\,dt = \sqrt{\sigma G S V_{\rm o}} \int_0^T |\dot{J}(t)|^{3/2}\,dt \qquad (9)$$

is applicable to any desired $J(t)$ waveform. In particular, we obtain for sinusoidal magnetization the expression

$$W_{\rm exc} = 8.76\sqrt{\sigma G S V_{\rm o}} J_{\rm p}^{3/2} f^{1/2} \qquad (10)$$

and for triangular magnetization

$$W_{\rm exc} = 8\sqrt{\sigma G S V_{\rm o}} J_{\rm p}^{3/2} f^{1/2}. \qquad (11)$$

The total loss is therefore obtained, according to (2) and (4), as

$$W = W_{\rm h} + (\pi^2/6)\sigma d^2 J_{\rm p}^2 f + 8.76\sqrt{\sigma G S V_{\rm o}} J_{\rm p}^{3/2} f^{1/2} \qquad (12)$$

and

$$W = W_{\rm h} + (4/3)\sigma d^2 J_{\rm p}^2 f + 8\sqrt{\sigma G S V_{\rm o}} J_{\rm p}^{3/2} f^{1/2} \qquad (13)$$

under sinusoidal and triangular $J(t)$, respectively. The latter case represents a lower limit for the loss figure.

The loss dependence on the sample geometry can be recognized by looking at the behavior of its components. $W_{\rm h}$ is geometry independent, exclusively being a material-related property, and $W_{\rm cl}(f)$ varies with the lamination thickness as d^2. For what concerns $W_{\rm exc}(f)$, it turns out that it may depend on d via the term $V_{\rm o} \cdot S$. Two extreme situations can be considered (see also the discussion in [4]). With size of magnetic objects small with respect to sample thickness (e.g., fine grained materials), $V_{\rm o} \cdot S$ is constant and $W_{\rm exc}(f)$ does not vary with d. With wide-spaced domain structures (e.g., grain-oriented alloys), a $\sqrt{d}$ dependence is predicted. In all cases, no role is played by the lamination width.

4) Parameters Identification: Whenever the condition (7) is verified, the prediction of the total loss for generic $J(t)$ in a soft lamination of given conductivity σ and cross-sectional area S requires the preemptive determination of $W_{\rm h}$ and $V_{\rm o}$ only. This amounts, according to (12), to the measurement of W under standard sinusoidal $J(t)$ at two different frequencies. Let us consider the typical experiment reported in Fig. 1, where the behavior of the quantity $W_{\rm dif}(f) = W(f) - W_{\rm cl}(f) = W_{\rm h} + W_{\rm exc}$, measured under sinusoidal flux in a grain-oriented Fe–Si lamination, is represented, together with its best straight fitting line, as provided by (12), as a function of $f^{1/2}$. We see that the $W_{\rm h}$ and $V_{\rm o}$ values are obtained from the intercept and the slope of the theoretical line, respectively, and, once introduced in the equation

$$W = W_{\rm h} + W_{\rm cl} + W_{\rm exc} = W_{\rm h} + \frac{\sigma d^2}{12}\int_0^T \dot{J}(t)^2\,{\rm d}t + \sqrt{\sigma G S V_{\rm o}} \int_0^T |\dot{J}(t)|^{3/2}\,{\rm d}t \qquad (14)$$

they suffice to fully predict the total loss under whatever $J(t)$ waveform. The predictive accuracy ensuing from the two-point measurement can be guessed from the scatter of the experimental data shown in Fig. 1(a). It can be improved by increasing the range of frequencies covered by preemptive testing. Fig. 2 provides an example of application of (14) to the prediction of the effect of third harmonic distortion on 50 Hz dynamic loss $W_{\rm dyn}(f) = W_{\rm cl}(f) + W_{\rm exc}(f)$, in a nonoriented Fe-(3 wt%) Si lamination. The third harmonic component, phase shifted by an angle φ_3 ranging between 0° and 180°, is in the ratio $J_3/J_1 = 0.1$ to the fundamental component and the peak magnetization value is kept constant at $J_{\rm p} = 1\,{\rm T}$. It is stressed that any novel prediction at a different $J_{\rm p}$ value requires novel experimental estimates of both $W_{\rm h}$ and $V_{\rm o}$.

If the approximation (7) does not hold, the expression (6) should be integrated in order to get the correct excess energy loss, giving

$$W_{\rm exc} = 2 n_{\rm o} V_{\rm o} J_{\rm p} \cdot \int_0^{\pi/2} \left(\sqrt{1 + \frac{8\sigma G S V_{\rm o}}{n_{\rm o}^2 V_{\rm o}^2} \pi f J_{\rm p} \cos\phi} - 1 \right) \cos\phi\, d\phi \qquad (15)$$

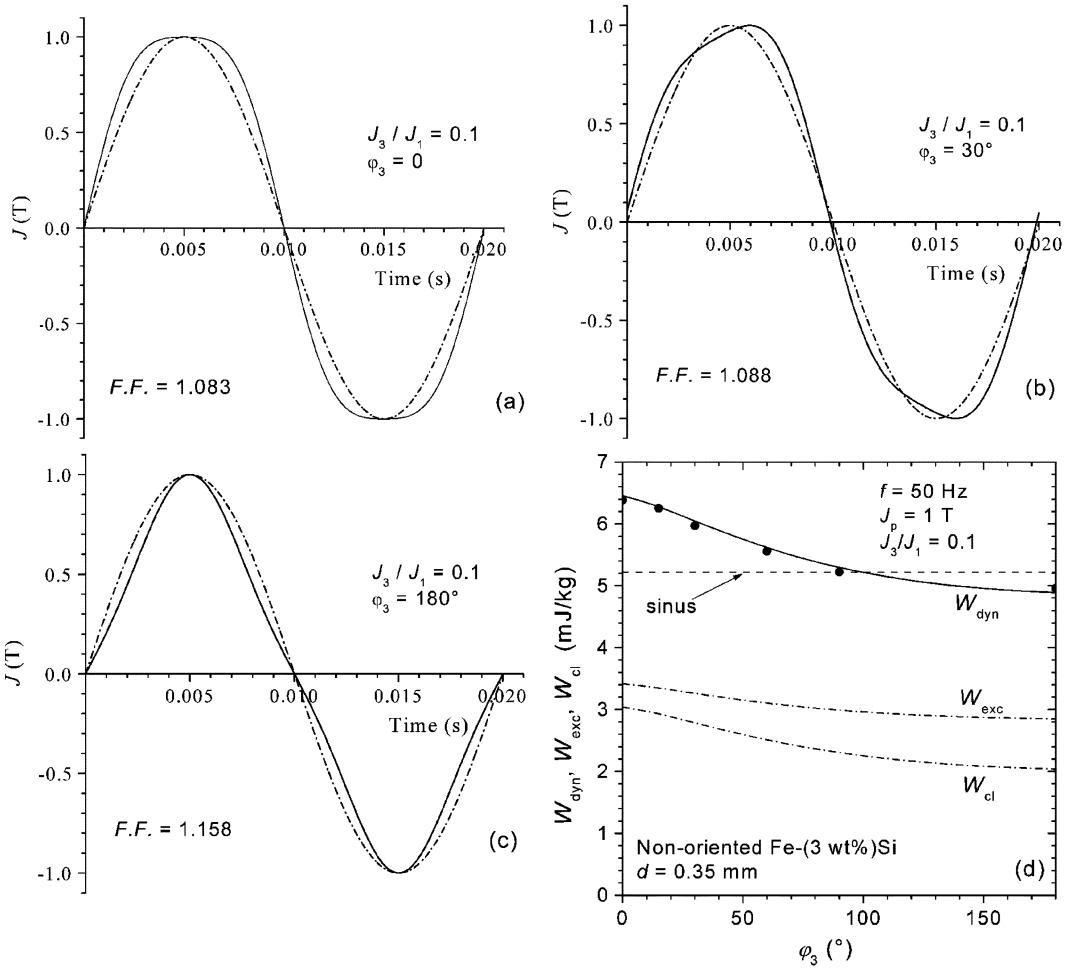


Fig. 2. Effect of third harmonic distortion, having fixed ratio $J_3/J_1 = 0.1$ to the fundamental component and variable phase φ_3, on the dynamic energy loss $W_{\rm dyn} = W_{\rm cl} + W_{\rm exc}$ in a nonoriented Fe-(3wt%)Si lamination at $f = 50$ Hz and $J_{\rm p} = 1$ T. Distorted $J(t)$ waveforms at different φ_3 values (solid lines) are compared with the reference sinusoidal $J(t)$ function (dashed line) in (a), (b), and (c). The theoretical behaviors of $W_{\rm cl}, W_{\rm exc}$, and $W_{\rm dyn}$ shown in (d), have been obtained following the experimental determination of $W_{\rm h}$ and the parameter $V_{\rm o}$, according to the procedure described in the text, and by application of (14). Theoretical (solid line) and experimental (full symbols) $W_{\rm dyn}$ values show excellent agreement. Notice that the evolution of the form factor FF around the value FF $= 1.1107$ is, for moderate distortions, only loosely related to the evolution of $W_{\rm dyn}$.

in case of sinusoidal $J(t)$, and

$$W_{\rm exc} = 2n_{\rm o}V_{\rm o}J_{\rm p}\left(\sqrt{1+\frac{16\sigma GSV_{\rm o}}{n_{\rm o}^2V_{\rm o}^2}fJ_{\rm p}}-1\right) \qquad (16)$$

for triangular $J(t)$.

Operating on the plot of $W_{\rm dif}$ versus $f^{1/2}$, by properly fitting the experimental points with (15) or (16) (according to the used waveform), one gets the parameters $n_{\rm o}, V_{\rm o}$, and $W_{\rm h}$. Again, it should be stressed that these parameters depend on the peak amplitude $J_{\rm p}$.

For a given peak amplitude $J_{\rm p}$, whichever is the waveshape $J(t)$, the actual $W_{\rm exc}, W_{\rm cl}$ terms can be calculated and the amount of the whole energy loss may be reconstructed.

As an example, Fig. 1(b) shows experimental results for sinusoidal $J(t)$, together with the (15) best fitting curve (solid line). This example shows that the deviation of the loci $f^{1/2} \rightarrow W_{\rm exc}$ from a straight line (broken line) is limited to a very narrow low frequency range.

This brings about a substantial simplification, because, for the magnetization rates associated with typical applicative frequencies (e.g., 50 Hz and higher), the condition (7) is recovered and the expression (6) for $p_{\rm exc}(t)$ becomes

$$p_{\rm exc}(t) = \sqrt{\sigma GSV_{\rm o}}|\dot{J}(t)|^{3/2} - (n_{\rm o}V_{\rm o}/2)|\dot{J}(t)| \qquad (17)$$

and consequently

$$W_{\rm exc} = \sqrt{\sigma GSV_{\rm o}}\int_0^T |\dot{J}(t)|^{3/2}\,dt - 2n_{\rm o}V_{\rm o}J_{\rm p}. \qquad (18)$$

The total loss under generic $J(t)$ can then be expressed, *at such frequencies*, as in (14)

$$W = W_{\rm h} + W_{\rm cl} + W_{\rm exc} = W_{\rm h} + \frac{\sigma d^2}{12}\int_0^T \dot{J}(t)^2\,dt + \left(\sqrt{\sigma GSV_{\rm o}}\int_0^T |\dot{J}(t)|^{3/2}\,dt - 2n_{\rm o}V_{\rm o}J_{\rm p}\right) \qquad (19)$$

but for the additional term $2n_{\rm o}V_{\rm o}J_{\rm p}$, independent of f.

Remarkably, the prediction of W by (19) at a given $J_{\rm p}$ value can still be obtained exploiting separate measurements of W

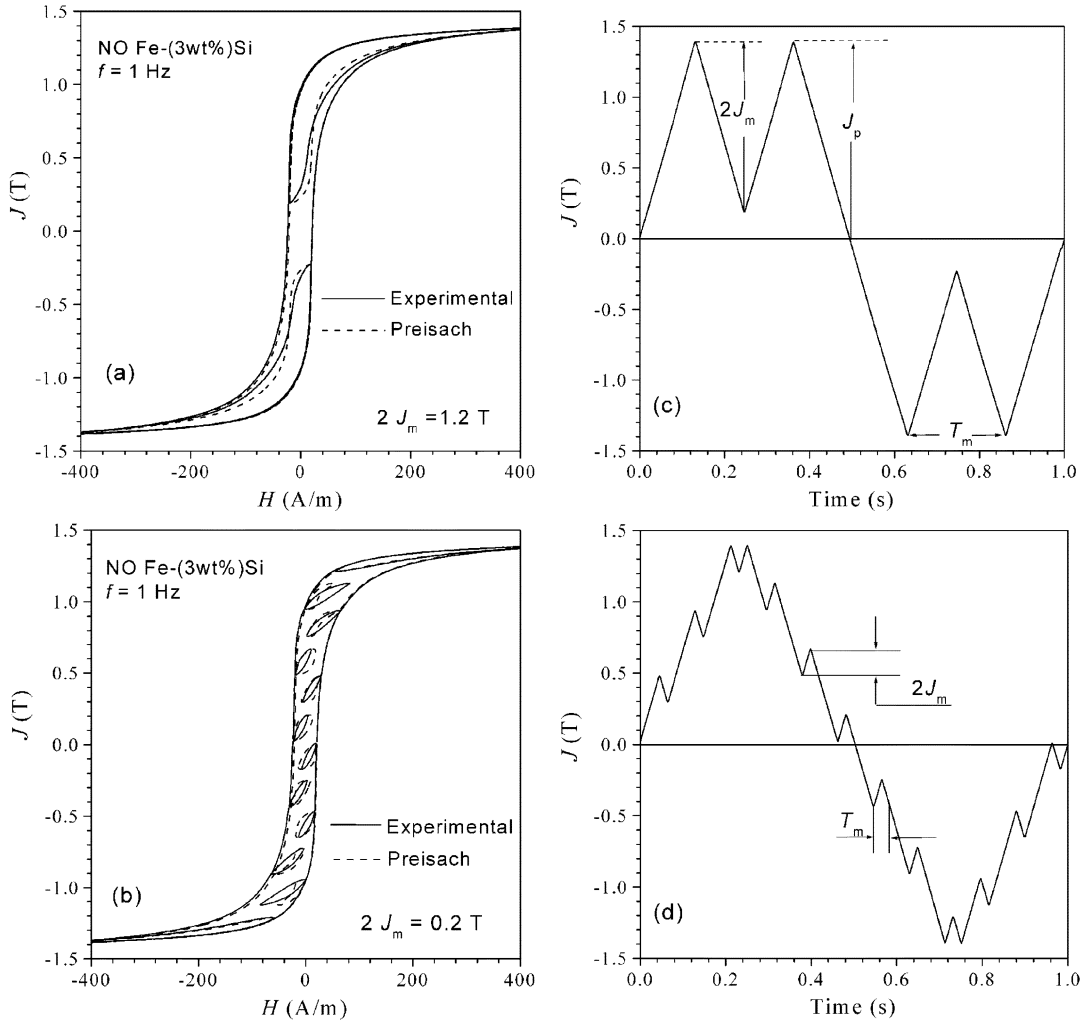


Fig. 3. Examples of composite experimental (solid lines) and reconstructed (dashed lines) static hysteresis loops at peak magnetization $J_{\rm p} = 1.4$ T in nonoriented Fe-(3 wt%)Si laminations (thickness 0.34 mm) generated by the $J(t)$ waveforms shown in (c) and (d). The minor loops have peak-to-peak amplitude $2\,J_{\rm m}$. The theoretical loops have been reconstructed by means of a Preisach model, using an experimental hysteresis loop taken at $J_{\rm p} = 1.5$ T as the sole input information and making suitable simplifying assumptions [18].

under sinusoidal $J(t)$ *at two different frequencies only*. If we write (19) as

$$W = W_{\rm h} + W_{\rm cl} + W_{\rm exc} = W_{\rm h1} + \frac{\sigma d^2}{12}\int_0^T \dot{J}(t)^2\,dt + \sqrt{\sigma G S V_{\rm o}}\int_0^T |\dot{J}(t)|^{3/2}\,dt \quad (20)$$

and take $J(t)$ sinusoidal, the quantity

$$W_{\rm h1} = W_{\rm h} - 2n_{\rm o}V_{\rm o}J_{\rm p} \quad (21)$$

is provided, as shown in Fig. 1(b), in the $(W_{\rm dif}, f^{1/2})$ plane by the intercept with the ordinate axis of the straight line of equation

$$W_{\rm dif}(f) = W_{\rm h1} + 8.76\sqrt{\sigma G S V_{\rm o}}J_{\rm p}^{3/2} f^{1/2} \quad (22)$$

having a slope proportional to $V_{\rm o}^{1/2}$. Substitution of the so found couple of parameters W_{h1} and $V_{\rm o}$ in (20) leads to the required prediction of the total loss W for arbitrary induction waveform at specified frequency and $J_{\rm p}$ values, irrespective of the restriction posed by (7).

B. Energy Losses With Arbitrary Flux Waveform and Minor Loops

We have shown that the loss prediction under arbitrary flux waveform and absence of minor loops can eventually be achieved in a simple way by mere preemptive determination of a couple of experimental loss values with sinusoidal $J(t)$, taken at different frequencies. In the presence of minor loops the whole phenomenology becomes more complex and the amount of information to be preemptively retrieved is larger, the objective always remaining that of exclusively using, for the sake of prediction, data obtained under standard measuring conditions. Again, we rely on the loss separation equations (1) and (2) and, accordingly, we carry out the procedure for the prediction of $W_{\rm cl}, W_{\rm h}$, and $W_{\rm exc}$. We immediately note that $W_{\rm cl}$ can *always* be calculated by means of (4) and we concentrate on the components $W_{\rm h}$ and $W_{\rm exc}$.

1) Quasi-Static Loss Component: Let us then consider a soft magnet subjected to a generic magnetization waveform $J(t)$ at the frequency f provided with $2n$ local minima. While in the absence of local minima the component $W_{\rm h}$ is independent of the specific $J(t)$ waveshape, now we have to deal with a behavior of the hysteresis loops like the one displayed in Fig. 3. We notice in

Fig. 3(b) how the minor loop area depends, for a same $J_{\rm m}$ value, on the position of the turning point along the major loop. Since we wish to carry out a minimum set of measurements, we need suitable quasi-static hysteresis loop modeling. Many prospective routes are open today for hysteresis modeling, ranging from truly empirical approaches to mathematically grounded theories [18]. In the present approach, a simplified Preisach model has been applied, by which the complex magnetic histories contained in the chosen representative array of $J(t)$ functions are described by making use of an experimentally determined limiting loop, that is, a major loop at which technical saturation is attained, as the sole input information [19]. In practice, a loop taken with $J_{\rm p} = 1.5$ T/1.6 T is appropriate in Fe–Si laminations. The modeling of the associated composite quasi-static hysteresis loop (major plus minor loops) has been carried out, and the loss components $W_{\rm h,M}$ (major loop area), $W_{\rm h,m}$ (cumulative areas of the minor loops), and their sum $W_{\rm h}$ have been determined.

A couple of thus calculated complex hysteresis histories with $2n$ minor loops are provided, for nonoriented Fe-(3 wt%)Si laminations, in Fig. 3, together with the pertaining time dependence of $J(t)$. Given the limited amount of input data, the chosen Preisach model may provide less than perfect loop shape reconstruction, but it eventually generates acceptable figures of the associated energy loss.

2) Excess Loss Component: We decompose first the ensemble made of the major loop of peak amplitude $J_{\rm p}$ and the array of $2n$ minor loops of peak-to-peak amplitude $2J_{{\rm m},i} (i = 1, 2, \ldots, 2n)$ and we perform the separate $W_{\rm exc}$ calculation for the major $(W_{\rm exc,M})$ and the minor $(W_{\rm exc,m})$ loops. All contributions are eventually summed up to obtain the global excess loss component. This operation amounts to a gross simplification of the problem, which compounds with the assumption of assigning definite identical *dynamic loss* properties to all minor loops provided with the same amplitude, independent of the position of their turning point along the major loop. Such properties are, in addition, identified with those of the loop centered at the origin having peak amplitude $J_{{\rm m},i}$. Altogether, these assumptions may appear to oversimplify the physical reality. However, they find their raison d'être in the demand for a simple, general, and reasonably accurate prediction method. A step forward in modeling, both in terms of physical detail and general validity would expectedly be accomplished by introducing the methods associated with the dynamic Preisach model (DPM) [20]. It is stressed that the here discussed loss model is nevertheless based on the very same, though simplified, physical assumptions. The drawback of DPM lies in its complexity and the computational burden, which could result in lack of acceptance by potential users.

a) Calculation of the Excess Loss Contribution $W_{\rm exc,M}$: Concerning the determination of $W_{\rm exc,M}$, we follow the procedure described in Section II-A. Thus, we only need, for given peak polarization amplitude $J_{\rm p}$, to experimentally determine the total loss value $W_{\rm M}^{(\sin)}$ under sinusoidal induction at two different frequencies. The resulting straight line in the $(W_{\rm dif}^{(\sin)}, f^{1/2})$ plane has, according to (22), intercept $W_{\rm h1,M}$ and slope $V_{\rm o}^{1/2}$. Using these two parameters, we calculate the quantity $W_{\rm h,M} + W_{\rm exc,M}$ under the prescribed waveform $J(t)$ at the desired frequency f as

$$W_{\rm h,M} + W_{\rm exc,M} = W_{\rm h1,M} + \sqrt{\sigma G S V_{\rm o}(J_{\rm p})} \int_{T_{\rm M}} |\dot{J}(t)|^{3/2}\, {\rm d}t. \quad (23)$$

Here, we have made explicit the $V_{\rm o}(J_{\rm p})$ dependence and the time integration of $|\dot{J}(t)|^{3/2}$ is extended only over the portion $T_{\rm M}$ of the period T which is not occupied by the minor loops.

b) Estimation of the Excess Energy Losses $W_{\rm exc,m}$: The estimation of the excess energy losses associated with the ensemble of minor loops is equally made by resorting to a two-frequency measurement. This regards now the total loss $W_{{\rm m},i}^{(\sin)}$ for individual symmetric loops of peak amplitude $J_{{\rm m},i}$, described under sinusoidal $J(t)$ law. Again, we achieve, using the $(W_{\rm dif}^{(\sin)}, f^{1/2})$ representation (Fig. 1), the value of the parameter $V_{\rm o}(J_{{\rm m},i})$. If all minor loops have the same amplitude, a single two-frequency test provides the required $V_{\rm o}$ value. To cover the most general case, where different minor loop amplitudes are involved (see, for example, the PWM supply experiment reported in Fig. 7), it is expedient to carry out the two-frequency test at selected $J_{\rm m}$ values. An experimental $V_{\rm o}(J_{\rm m})$ function curve can be obtained in this way. An example of such a curve is provided, for the presently investigated nonoriented Fe–Si laminations, in Fig. 5. To simplify the matter, we assume that (7) applies and we calculate the excess loss associated with the ith minor loop $(W_{{\rm exc,m},i})$ by using (9), written as

$$W_{{\rm exc,m},i} = \sqrt{\sigma G S V_{\rm o}(J_{{\rm m},i})} \int_{T_{{\rm m},i}} |\dot{J}(t)|^{3/2}\, {\rm d}t \quad (24)$$

where the integration is made over the associated ith time interval of duration $T_{{\rm m},i}$. The global contribution of the $2n$ minor loops will be

$$W_{\rm exc,m} = \sum_{i=1}^{2n} W_{{\rm exc,m},i}. \quad (25)$$

The approximations we have made ($W_{{\rm exc,m},i}^{(\sin)}$ independent on minor loop position) simplify the analytical approach and, regarding only a portion of the total loss, are expected to introduce acceptably small uncertainty in the prediction.

We can now gather all the contributions and eventually obtain the expression for the total loss at a given frequency f in the presence of minor loops

$$W = W_{\rm h} + W_{\rm exc,M} + W_{\rm exc,m} + \frac{\sigma d^2}{12} \int_0^T \dot{J}(t)^2\, dt \quad (26)$$

where the whole static loss $W_{\rm h} = W_{\rm h,M} + W_{\rm h,m}$ can be obtained by means of Preisach modeling (or other more or less empirical modeling), exploiting the experimental determination of a major symmetric hysteresis loop at technically high $J_{\rm p}$ values. The quasi-static loss term $W_{\rm h,M}$ is known either from direct measurement or Preisach modeling. By introducing it in (23), one

can calculate $W_{\mathrm{exc,M}}$, while the global excess loss $W_{\mathrm{exc,m}}$ associated with the minor loops is provided by (25).

III. Experimental Procedure

Energy loss and hysteresis loop measurements have been carried out in nonoriented Fe-(3 wt%)Si laminations (thickness 0.348 mm, resistivity 56×10^{-8} Ω·m, average grain size 230 μm) in the frequency range 0.5–400 Hz under sinusoidal, triangular, and generic $J(t)$ waveform. Longitudinally cut strips have been tested with an Epstein frame, by means of a designed-on-purpose hysteresisgraph-wattmeter, endowed with digital control of the flux waveform. A feedback algorithm iteratively calculates the voltage to be supplied by the arbitrary function generator at the input of the primary circuit, based on the difference detected, at each instant of time, between actual and desired induction and actual and desired secondary voltage. Two-channel synchronous acquisition of the H and $\mathrm{d}B/\mathrm{d}t$ signals is performed via a 150 Msample/s digital oscilloscope, with minimum 12 bit effective vertical resolution and 5000 points per period. Calibration of the measuring setup is accomplished by comparison with a conventional reference wattmeter, tested and assessed through international intercomparisons [21].

A. Loss Separation and Parameter Identification

Fig. 4(a) shows the experimentally found frequency behavior of the magnetic energy loss under sinusoidal and triangular induction waveform at peak magnetization $J_{\mathrm{p}} = 1.4\,\mathrm{T}$. The fitting lines have been predicted according to the method outlined in the previous section, focused on the loss separation provided by (12) and (13). Fig. 4(b) illustrates the loss decomposition, where the classical loss W_{cl} is calculated by (4) and subtracted to the total loss W. The quantity $W_{\mathrm{dif}} = W - W_{\mathrm{cl}} = W_{\mathrm{h}} + W_{\mathrm{exc}}$ is here represented as a function of $\sqrt{f}$. We find by this representation that we fall in the case where W_{dif} exhibits a deviation from the $\sqrt{f}$ dependence at low frequencies. We make then best fitting of W_{dif} in Fig. 4(b) and of W in Fig. 4(a) by applying (15) (sinusoidal $J(t)$) and (16) (triangular $J(t)$). We notice that W_{dif} becomes proportional to $\sqrt{f}$ beyond about 10 Hz. At frequencies of practical interest, the whole treatment can then be simplified with the use of (22) and (20) and it is verified that the loss prediction under whatever $J(t)$ function with no local minima requires experimental determination of W with sinusoidal $J(t)$ at two frequencies only, providing for the parameters W_{h1} and V_{o}. An example of successful application of this rule was provided in Fig. 2.

B. First Example

Let us turn our attention to the losses in the presence of minor loops. First, we consider the use of (26) in the specific case illustrated in Fig. 3, according to the following conditions: $J_{\mathrm{p}} = 1.4\,\mathrm{T}$, all minor loops of same peak-to-peak amplitude $2J_{\mathrm{m}}$ and variable number $2n = 2, 4, \ldots, 12$, with constant value of the product $2n \times J_{\mathrm{m}} = 1.2$ T. The time derivative of the induction is kept constant along the period, its value depending on the number of minor loops as $|\dot{J}(t)| = 4f(J_{\mathrm{p}} + 2nJ_{\mathrm{m}})$. Then we analyze the various terms of (26), by noting first that, as remarked in Section II-B, the hysteresis loss component $W_{\mathrm{h,M}} + \sum_{i=1}^{2n} W_{\mathrm{h,m},i}$ can be calculated by appropriate quasi-static hysteresis modeling. An example of application of the Preisach model to the present case is reported in Fig. 3. The term $W_{\mathrm{exc,M}}$, pertaining to the major loop, is obtained by means of (23) as

$$W_{\mathrm{exc,M}} = (W_{\mathrm{h1,M}} - W_{\mathrm{h,M}}) + 8\sqrt{\sigma G S V_{\mathrm{o}}(J_{\mathrm{p}})} \cdot (J_{\mathrm{p}} + 2nJ_{\mathrm{m}})^{3/2} \cdot f^{1/2} \cdot (1 - 2nT_{\mathrm{m}}/T) \quad (27)$$

where T_{m} is the duration of each minor loop.

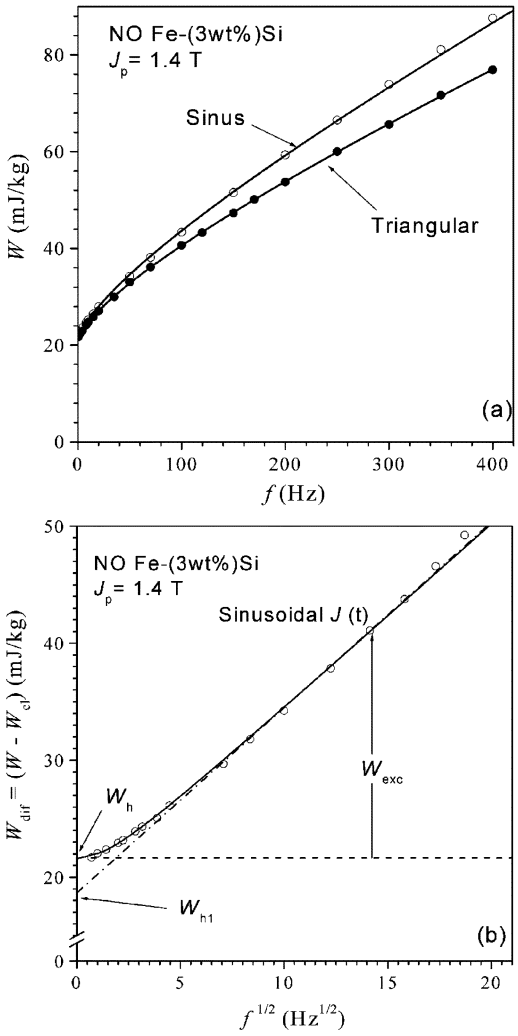


Fig. 4. Energy loss per cycle W and its analysis in a nonoriented Fe-(3wt%)Si lamination. It is shown in (a) that, by changing the $J(t)$ waveform from sinusoidal to triangular, the total loss is decreased, as predicted by the theory. The solid lines are calculated by means of the equation $W = W_{\mathrm{h}} + W_{\mathrm{cl}} + W_{\mathrm{exc}}$, with W_{cl} given by (4), and W_{exc} and W_{h} obtained by means of the procedure sketched in (b). Here, the experimental quantity $W_{\mathrm{dif}} = W - W_{\mathrm{cl}} = W_{\mathrm{h}} + W_{\mathrm{exc}}$ is plotted as a function of $\sqrt{f}$ and fitted using (15) (solid line). Beyond the very low frequency region, (15) simplifies into (18) and W_{dif} is consequently provided by (22). This results in the dash-dot straight fitting line, by which the two parameters W_{h1} and V_{o} are determined and used, once introduced in (20), to predict the total loss under generic $J(t)$ waveform. Two independent loss measurements at different frequencies under sinusoidal $J(t)$ suffice to make such a general prediction.

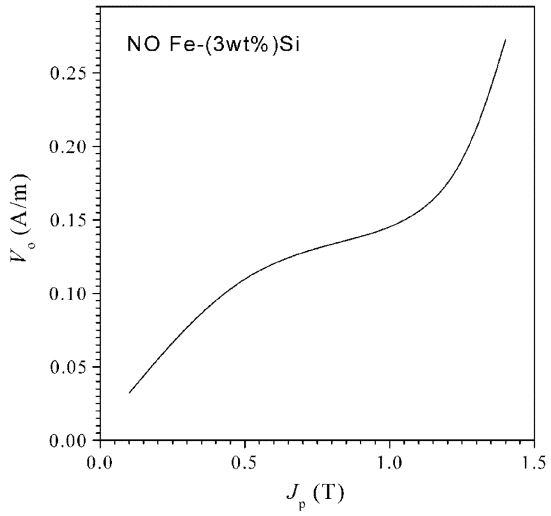


Fig. 5. Behavior of the statistical parameter $V_o(J_p)$ in the investigated nonoriented Fe–Si laminations.

The excess loss contribution associated with the minor loops is derived from (24) and (25), according to the approximations therein contained, as

$$W_{\mathrm{exc,m}} = \sum_{i=1}^{2n} W_{\mathrm{exc,m},i} = (2n) \times 8\sqrt{\sigma G S V_{\mathrm{o}}(J_{\mathrm{m}})} \cdot (J_{\mathrm{p}} + 2nJ_{\mathrm{m}})^{3/2} f^{1/2} (T_{\mathrm{m}}/T). \quad (28)$$

The classical loss is calculated by means of (4) as

$$W_{\mathrm{cl}} = (4/3)\sigma d^2 (J_{\mathrm{p}} + 2nJ_{\mathrm{m}})^2 f. \quad (29)$$

To remark that the parameter $V_{\mathrm{o}}(J_{\mathrm{p}})$, related to the statistical properties of the magnetization process, in particular to the distribution of the local coercive fields, is an increasing function of J_{p}, as illustrated for the present nonoriented Fe–Si lamination in Fig. 5. By introducing the results provided by (27)–(29) in (26), we arrive at the prediction shown in Fig. 6, which comfortably compares with the experiments.

C. Second Example

Another application of the model is illustrated in Figs. 7 and 8. It regards a typical condition arising with a two-level PWM supply. This is characterized by the following parameters: ratio of switching frequency to modulation frequency $m_f = f_s/f = 21$; modulation index $m_a = 0.6, 0.7, \ldots, 1$; peak amplitude of the magnetic polarization $J_{\mathrm{p}} = 1\,\mathrm{T}$ and $J_{\mathrm{p}} = 1.4\,\mathrm{T}$; modulation frequency $f = 50$ Hz and $f = 100$ Hz. The time derivative of the induction is constant along the period, its value depending on the values assigned to m_f, m_a, and J_{p} according to the equation

$$|\dot{J}(t)| = 4J_{\mathrm{p}} \times g_{\mathrm{M}}(m_a, m_f) f \quad (30)$$

where

$$g_{\mathrm{M}}(m_a, m_f) \cong \frac{m_f}{1 + 2m_a \times \sum_{i=1}^{(m_f-1)/2} \sin[2\pi(3/4 + i - 1)/m_f]}. \quad (31)$$

We analyze, as done in the previous case, the various terms appearing in (26). The hysteresis loss component W_{h} is calculated

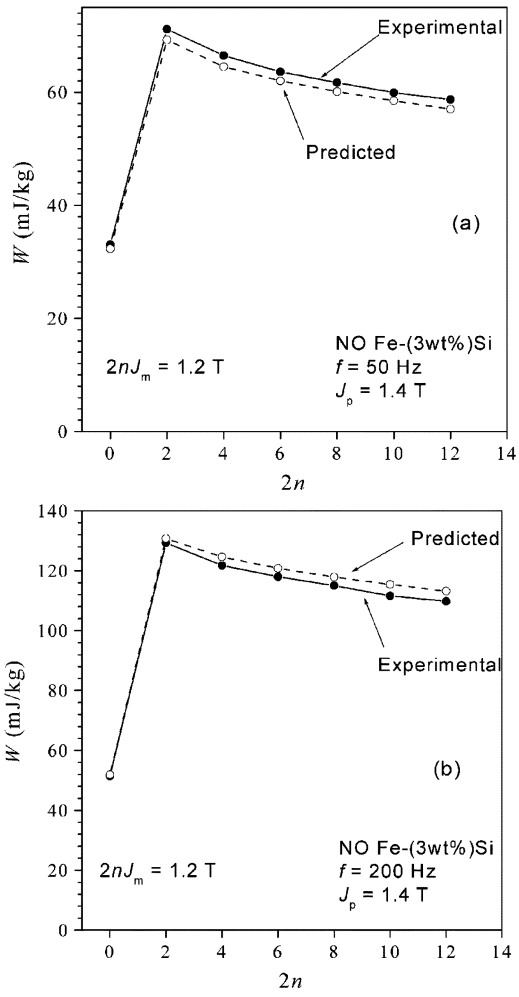


Fig. 6. Evolution of the energy loss with the number of minor loops in a nonoriented Fe-(3wt%)Si lamination under controlled constant magnetization rate $|\dot{J}(t)| = 4f(J_{\mathrm{p}} + 2J_{\mathrm{m}})$, with $J_{\mathrm{p}} = 1.4$ T and $2nJ_{\mathrm{m}} = 1.2$ T. Examples of associated composite hysteresis loops (for $n = 2$ and $n = 6$) are shown in Fig. 3. The total loss prediction is made for $f = 50$ Hz and $f = 200$ Hz by means of (26), specific to this case through (27)–(29).

by Preisach modeling. Fig. 7(b) provides the result of such a calculation for $J_{\mathrm{p}} = 1$ T. The term $W_{\mathrm{exc,M}}$, pertaining to the major loop, is obtained by means of (23), in terms of the parameters m_a and m_f

$$W_{\mathrm{exc,M}} = (W_{\mathrm{h1,M}} - W_{\mathrm{h,M}}) + 8\sqrt{\sigma G S V_{\mathrm{o}}(J_{\mathrm{p}})} J_{\mathrm{p}}^{3/2} \sqrt{g_{\mathrm{M}}(m_a, m_f)} \sqrt{f}. \quad (32)$$

The excess loss contribution associated with the minor loops is derived from (24) and (25)

$$W_{\mathrm{exc,\,m}} = 2 \sum_{i=1}^{(m_f-1)/2} W_{\mathrm{exc,m},i} = 2 \sum_{i=1}^{(m_f-1)/2} 8\sqrt{\sigma G S V_{\mathrm{o}}(J_{\mathrm{m},i})} J_{\mathrm{m},i}^{3/2} \sqrt{g_{\mathrm{m},i}(m_a, m_f)} \sqrt{f} \quad (33)$$

where

$$g_{\mathrm{m},i}(m_a, m_f) \cong \frac{m_f}{1 - m_a \times \sin[2\pi(3/4 + i - 1)/m_f]} \quad (34)$$

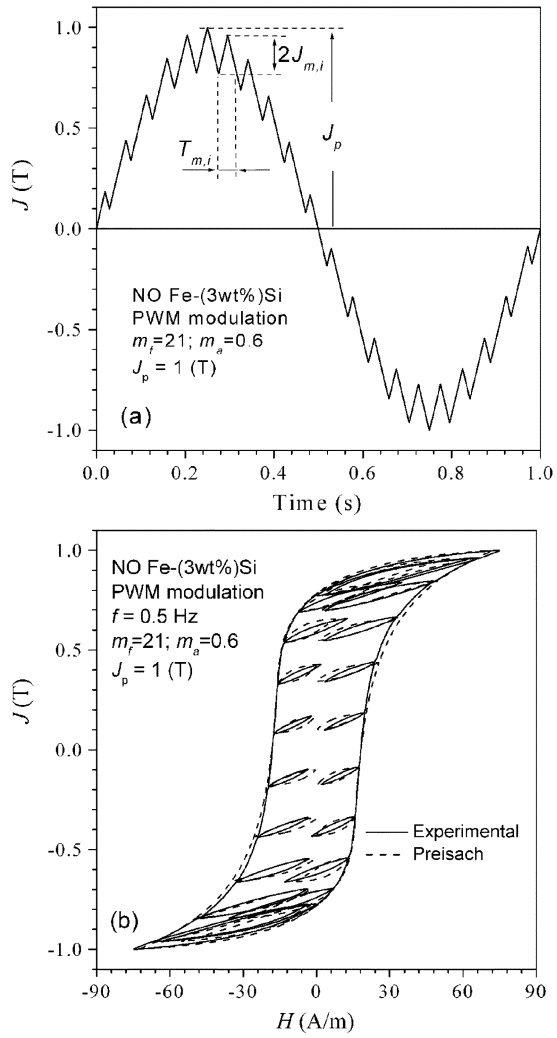


Fig. 7. Magnetic polarization $J(t)$ and hysteresis loop behavior with a two-level PWM supply. This example is characterized by modulation frequency ratio $m_f = 21$ and modulation index $m_a = 0.6$. Peak polarization value $J_P = 1$ T. Corresponding experimental (solid lines) and reconstructed (dashed lines) quasi-static hysteresis loops in nonoriented Fe-(3 wt%)Si laminations (thickness 0.34 mm) are shown in (b). The loop reconstruction has been made as in Fig. 3.

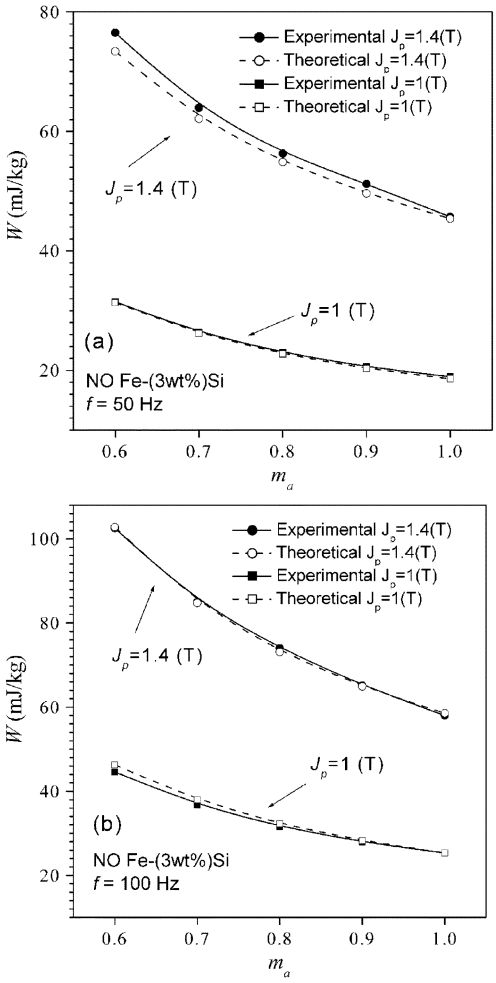


Fig. 8. Experimental and predicted energy loss behavior under two-level PWM supply with modulation frequency ratio $m_f = 21$, modulation index m_a varying between 0.6 and 1, and frequency (a) $f = 50$ Hz and (b) $f = 100$ Hz. An example of associated quasi-static composite hysteresis loop ($m_a = 0.6$, $J_p = 1$ T) is shown in Fig. 7(b). The total loss prediction is based, as always, on (26), formulated in terms of modulation parameters through (32), (33), and (36).

and

$$J_{m,i} = J_p \frac{g_M(m_a, m_f)}{g_{m,i}(m_a, m_f)}. \tag{35}$$

The classical loss is calculated by means of (4) as

$$W_{cl} = (4/3)\sigma d^2 J_p^2 g_M(m_a, m_f)^2 f. \tag{36}$$

Introducing the results provided by (30)–(36) in (26), the prediction shown in Fig. 8 is obtained, in good agreement with the experiments.

IV. Conclusion

A method has been developed for the prediction of the energy losses in soft magnetic laminations subjected to arbitrary induction waveform. The approach here proposed, which is based on the concept of loss separation and the statistical theory of losses, allows for prediction in the presence of local minima in the time dependence of the induction, that is minor hysteresis loops. It is shown that in this case, with a composite hysteresis curve made of a major loop and $2n$ minor loops of peak polarization J_p and J_m, respectively, the minimum required input information consists in:

1) experimental knowledge of a major quasi-static hysteresis loop, taken at sufficiently high peak polarization values (typically, 1.5–1.6 T in nonoriented Fe–Si alloys);
2) value of the energy loss, measured for the two involved polarization values J_p and J_m at two different frequencies, under standard testing conditions (e.g., sinusoidal induction).

If the $J(t)$ waveform implies the existence of several different minor loop amplitudes, two-frequency loss tests at selected J_m values shall be carried out.

References

[1] C. Cester, A. Kedous-Lebouc, and B. Cornut, "Iron loss under practical working conditions of a PWM powered induction motor," *IEEE Trans. Magn.*, vol. 33, pp. 3766–3768, Sept. 1997.

[2] A. Boglietti, P. Ferraris, M. Lazzari, and M. Pastorelli, "Iron loss measurements with inverter supply: A first discussion to define a standard methodology," *IEEE Trans. Magn.*, vol. 31, pp. 4006–4008, Nov. 1995.
[3] F. Fiorillo and A. Novikov, "An improved approach to power losses in magnetic laminations under nonsinusoidal induction waveform," *IEEE Trans. Magn.*, vol. 26, pp. 2904–2910, Sept. 1990.
[4] G. Bertotti, "Physical interpretation of eddy current losses in ferromagnetic materials," *J. Appl. Phys.*, vol. 57, pp. 2110–2126, 1985.
[5] F. Fiorillo and A. Novikov, "Power losses under sinusoidal, trapezoidal and distorted induction waveform," *IEEE Trans. Magn.*, vol. 26, pp. 2559–2561, Sept. 1990.
[6] M. Amar and R. Kaczmarek, "A general formula for prediction of iron losses under nonsinusoidal voltage waveform," *IEEE Trans. Magn.*, vol. 31, pp. 2504–2509, Sept. 1995.
[7] K. Atallah and D. Howe, "The calculation of iron losses in brushless permanent magnet DC motors," *J. Magn. Magn. Mater.*, vol. 133, pp. 578–582, 1994.
[8] A. Boglietti, M. Chiampi, M. Repetto, O. Bottauscio, and D. Chiarabaglio, "Loss separation analysis in ferromagnetic sheets under PWM inverter supply," *IEEE Trans. Magn.*, vol. 34, pp. 1240–1242, July 1998.
[9] E. Ferrara, C. De Luigi, C. Beatrice, C. Appino, and F. Fiorillo, "Energy loss vs. magnetizing frequency in field-annealed nanocrystalline alloys," *J. Magn. Magn. Mater.*, vol. 215–216, pp. 466–468, June 2000.
[10] T. Nakata, Y. Ishihara, and M. Nakano, "Iron losses of silicon steel core produced by distorted flux," *Elect. Eng. Jpn.*, vol. 90, pp. 10–20, 1970.
[11] J. D. Lavers, P. P. Biringer, and H. Hollitscher, "A simple method of estimating the minor loop hysteresis loss in thin laminations," *IEEE Trans. Magn.*, vol. 14, pp. 386–388, Sept. 1978.
[12] P. Rupanagunta, J. S. Hsu, and W. F. Weldon, "Determination of iron core losses under influence of third-harmonic flux component," *IEEE Trans. Magn.*, vol. 27, pp. 768–777, Mar. 1991.
[13] M. Akroune, R. Aouli, M. A. Dami, and A. Mouillet, "Characterization of nonoriented electric alloys under non conventional conditions," *Proc. Inst. Elect. Eng.—Sci. Meas. Technol.*, vol. 143, pp. 35–40, 1996.
[14] C. Cho, D. Son, and Y. Cho, "Core loss analysis of nonoriented electrical steel under magnetic induction including higher harmonics," *J. Magn.*, vol. 6, p. 66, 2001.
[15] M. Lancarotte and A. de A. Penteado, Jr., "Estimation of core losses under sinusoidal or nonsinusoidal induction by analysis of magnetization rate," *IEEE Trans. Energy Conversion*, vol. 16, pp. 174–179, June 2001.
[16] G. Bertotti, *Hysteresis in Magnetism*. San Diego, CA: Academic, 1998.
[17] L. Dupre, G. Bertotti, and J. Melkebeek, "Dynamic Preisach model and energy dissipation in soft magnetic materials," *IEEE Trans. Magn.*, vol. 34, pp. 1168–1170, July 1998.
[18] I. D. Mayergoyz, *Mathematical Models of Hysteresis*. New York: Springer-Verlag, 1991.
[19] C. Ragusa, "An analytical method for the identification of the Preisach distribution function," *J. Magn. Magn. Mater.*, vol. 254–255, pp. 259–261, 2003.
[20] G. Bertotti, "Dynamic generalization of the scalar Preisach model of hysteresis," *IEEE Trans. Magn.*, vol. 28, pp. 2559–2601, Sept. 1992.
[21] J. Sievert, H. Ahlers, F. Fiorillo, L. Rocchino, M. Hall, and L. Henderson, PTB-Bericht E-74, pp. 1–28, 2001.